energies

MDPI

Article

Metal-Free Modified Boron Nitride for Enhanced CO_2 Capture

Fereshteh Hojatisaeidi [1], Mauro Mureddu [2], Federica Dessì [2], Geraldine Durand [1,3] and Basudeb Saha [1,*]

1 School of Engineering, London South Bank University, 103 Borough Road, London SE1 0AA, UK; hojatisf@lsbu.ac.uk (F.H.); geraldine.durand@twi.co.uk (G.D.)
2 Sotacarbo S.p.A. Grande Miniera di Serbariu, 09013 Carbonia (CA), Italy; mauro.mureddu@sotacarbo.it (M.M.); federica.dessi@sotacarbo.it (F.D.)
3 The Welding Institute, Granta Park, Great Abington, Cambridge CB21 6AL, UK
* Correspondence: b.saha@lsbu.ac.uk; Tel.: +44-(0)20-7815-7190; Fax: +44-(0)20-7815-7699

Received: 28 November 2019; Accepted: 21 January 2020; Published: 23 January 2020

Abstract: Porous boron nitride is a new class of solid adsorbent with applications in CO_2 capture. In order to further enhance the adsorption capacities of materials, new strategies such as porosity tuning, element doping and surface modification have been taken into account. In this work, metal-free modification of porous boron nitride (BN) has been prepared by a structure directing agent via simple heat treatment under N_2 flow. We have demonstrated that textural properties of BN play a pivotal role in CO_2 adsorption behavior. Therefore, addition of a triblock copolymer surfactant (P123) has been adopted to improve the pore ordering and textural properties of porous BN and its influence on the morphological and structural properties of pristine BN has been characterized. The obtained BN-P123 exhibits a high surface area of 476 m^2/g, a large pore volume of 0.83 cm^3/g with an abundance of micropores. More importantly, after modification with P123 copolymer, the capacity of pure CO_2 on porous BN has improved by about 34.5% compared to pristine BN (2.69 mmol/g for BN-P123 vs. 2.00 mmol/g for pristine BN under ambient condition). The unique characteristics of boron nitride opens up new routes for designing porous BN, which could be employed for optimizing CO_2 adsorption.

Keywords: porous boron nitride; metal-free modification; structure directing agent; CO_2 capture

1. Introduction

Over the last decades, climate change has become a global challenge for countries across the world [1]. Carbon capture and storage (CCS) is expected to play a substantial role in meeting the global warming targets set by the Inter-governmental Panel on Climate Change (IPCC) [2]. It is a promising option to maintain fossil fuels as a global central energy contributor and is expected to progress in lab scale, pilot scale, demonstration scale and commercial scale [3]. Chemical absorption technology, which has been used to remove CO_2 from natural gas, is reached to the commercial phase of development and several pilot-scale projects have been conducted since decades ago [4,5]. To date, the capture technologies that have been demonstrated in pilot plant scale or higher are classified as (i) post-combustion, (ii) pre-combustion, and (iii) oxy-fuel combustion [6]. Among the current available technologies, CO_2 capture from post-combustion emission gases is the most common technology in power plants and industries. Effective methods to separate, capture, store, and convert CO_2 have attracted increasing attention [7]. The current technology for CO_2 capture is based on absorption in aqueous organic amines [8]. However, the intensive energy consumption, equipment corrosion and toxicity, make exploration of new materials for CO_2 capture highly demanding [9].

Solid adsorption is an alternative process to solvent-based chemisorption, which can be applied for a wide range of temperature and pressure conditions. Also, it can be designed for both post-combustion and pre-combustion applications. One of the challenges in this area relates to the manufacturing of new adsorbents that enables enhancing good diffusion kinetics and providing improved performance [10]. In this regards, porous materials with high porosity, chemical and thermal stability are promising solid adsorbents for capturing CO_2 [11,12]. Among various kinds of porous materials, such as zeolites [13,14], porous polymers [15], metal-organic framework [16,17] and activated carbons [18], porous BN has become one of the new classes of CO_2 adsorbents. Due to intrinsic properties of boron nitride such as high thermal and oxidation stability, large surface area, and polarity, porous boron nitride is a desired alternative for CO_2 capture [19,20]. However, according to theoretical and experimental works, the interaction between pristine BN and CO_2 is very weak due to electron deficient nature of boron atoms and the Lewis acidic nature of CO_2 [21–23]. To overcome such disadvantages, some strategies in view of tuning the structure, pore size and charge state of the BN have been studied. Nag et al. [24] made a few-layered BN by controlled chemical synthesis. Similarly, the effects of different proportions of urea on the number of BN layers indicate that the sample with the lowest layer thickness shows a high CO_2 uptake. Xiao et al. [25] reported a few layered porous boron nitride nanosheets (BNNs) by using magnesium diboride (MgB_2) as a dynamic template. However, the CO_2 uptake of their work was relatively low (0.45 mmol/g), while it demonstrated excellent selectivity of CO_2 over N_2. Yang et al. [26] developed a three dimensional (3D) functionalized porous BN with flower-like morphology and high specific surface area ≈114 m^2/g, and it shows 1.69 mmol/g CO_2 capture capacity at 1 bar and 273 K. It is also interesting to note that in most studies, element doping, and surface functionalization of boron nitride is critical to increase the CO_2 adsorption capacity. For instance, Chen et al. [27] produced ultrahigh microporous volume of boron carbon nitride (BCN) by doping carbon into hexagonal structure of BN. The performance of BCN material displays increased relative to pure BN for CO_2 uptake and reached up to 3.91 mmol/g at 298 K and ambient pressure. In addition, Huang et al. [28] enriched the interaction between electron-deficient boron atoms in BN and CO_2 molecules by aminopolymer-functionalized BN nanosheets. Therefore, porous structure and surface chemistry features of BN-based materials play crucial roles in CO_2 adsorption performance and it remains a challenge to control the parameters of boron nitride porosity and develop novel structures with high capacitive performance for carbon capture.

In this work, with the aim of achieving high CO_2 adsorption capacity of porous BN through tuning the porosity, BN structure has been modified in the presence of P123 as a structure directing agent. The synthesized BN-P123 possesses high specific surface area and pore volume compared to pristine BN, which results in an enhanced CO_2 adsorption capacity.

2. Materials and Methods

Metal-free modified BN was synthesized on a two-step method of solvent evaporation and high thermal decomposition [29]. Boric acid (ACS reagent, Sigma-Aldrich), urea (for synthesis, Sigma-Aldrich) and Pluronic P123 triblock copolymers ($M_n \approx 5800$, Sigma-Aldrich) based on poly (ethylene glycol)-poly (propylene glycol)-poly (ethylene glycol) were used as raw materials. In detail, boric acid and urea with molar ratio 1:30 were added into 50 mL deionized water. Then 0.5 g P123 was introduced into the mixture solution and heated up at 338 K under vigorous stirring. A white precipitate was obtained after complete evaporation of water at that temperature. Afterwards, the precursor was dried into the oven for 24 h and annealed at 1173 K under N_2 gas (the flow rate was 150 mL/min) for 3 h. Finally, modified porous BN was collected and marked as BN-P123. For comparison, pristine BN was also prepared following the same procedure without adding any surfactant.

The morphology of samples was collected scanning electron microscope (SEM, PEMTRON PS-230) in secondary electron mode (SE detector) at 10 kV. The microscope was equipped with an energy-dispersive X-ray (EDX, OXFORD X-act) with energy resolution at 5.9 keV for the local elemental

analysis. The samples were ground, deposited on carbon tape, and coated (BIO-RAD sputter coater) with gold to reduce charging in the microscope.

X-ray diffraction (XRD) was performed to evaluate the structural properties using an X-ray diffractometer (Bruker D8 Advance) in reflection mode. The diffraction patterns run at an anode voltage of 40 kV and an emission current of 40 mA using monochromatic Cu Kα radiation (λ = 1.5418 Å). The intermolecular bonding and chemical properties of the materials were characterized by Fourier-transform infrared (FTIR) spectroscopy. The spectra were recorded on a Nicolet Avatar 370 spectrometer from 4000 to 400 cm^{-1} using KBr pellets at room temperature. Optical absorption measurement (SHIMADZU UV-1800) was performed. Prior to the measurement, the powder materials were dispersed in water (50 mg of samples in 25 mL water at room temperature). The thermal stability of samples was performed using thermal gravimetric analysis (TGA), Ultra micro balance, Mettler Toledo. An alumina pan was loaded with 5–10 mg of sample material and heated from room temperature to 1273 K at a rate of 10 K/min in air atmosphere.

Nitrogen isotherms were obtained using a porosity analyzer (Micromeritics ASAP2060) at 77 K. The surface areas of the samples were calculated using the Brunauer-Emmett-Teller (BET) method. The total volume of pores was calculated using the software from the BJH adsorption calculation. The CO_2 adsorption and desorption performance were evaluated with a TGA/DSC 3+ micro balance, Mettler Toledo. The CO_2 capture capacity of the sorbents were determined by measuring the mass uptake of the sample during the CO_2 adsorption.

3. Results and Discussion

3.1. Sample Characterisation

The morphology of samples was studied using scanning electron microscopy (SEM). The pristine BN exhibited an ultrathin flake-like morphology, as displayed in (Figure 1a,b). BN-P123 presented a cloud-like sheet structure with interconnected network of porous structure (Figure 1c,d). Moreover, the formation of pristine BN and BN-P123 were studied by EDX and elemental mapping (Figure 2a,b). It is obvious that the product is mainly comprised of boron (B), nitrogen (N) and oxygen (O). As shown in Figure 2b, BN-P123 has very little increase in oxygen content compared to pristine BN. This is due to the introduction of P123 into BN formation.

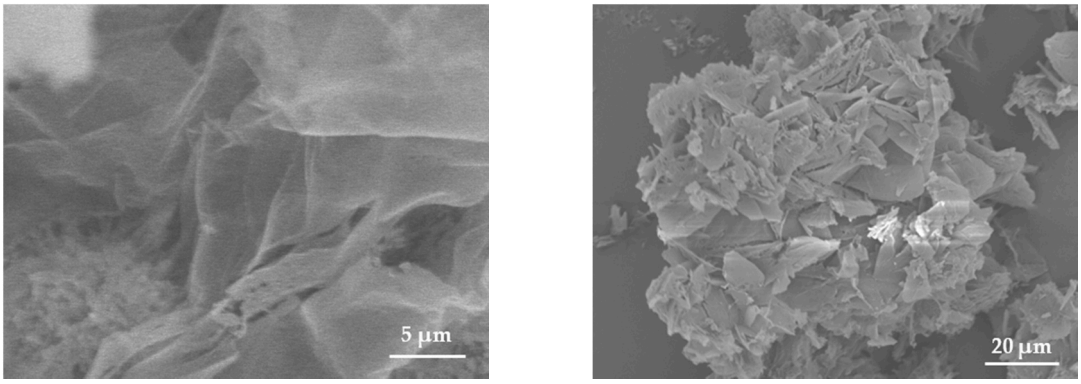

(**a**) (**b**)

Figure 1. *Cont.*

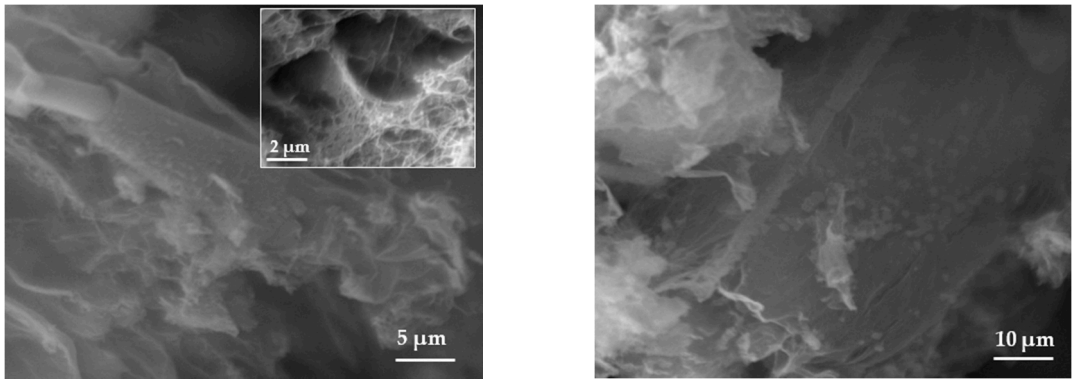

(**c**) (**d**)

Figure 1. SEM images of (**a**,**b**) pristine BN; (**c**,**d**) BN-P123.The insert shows the interconnected porous structure.

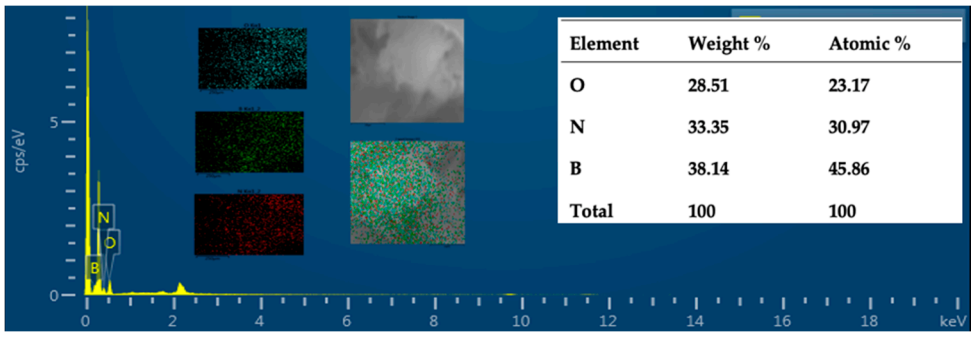

(**a**)

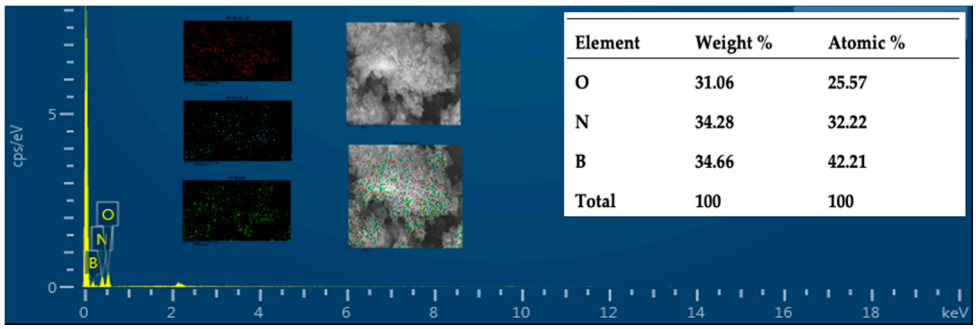

(**b**)

Figure 2. EDX spectra of (**a**) pristine BN; (**b**) BN-P123 and the insert show the elemental mapping and corresponding atomic % of elements.

The structure of samples was analysed and Figure 3a depicts the XRD patterns of the prepared samples. The results show two characteristic peaks around ≈25° and ≈42° which are attributed to the (002) and (100) crystal planes of hexagonal boron nitride, respectively [30]. Additionally, the peaks of both samples confirmed the poor crystallization with the presence of turbostratic material. Compared with pristine BN, the (002) diffraction peaks of BN-P123 shifted to a lower angle, which promote more disordered hexagonal boron nitride (h-BN) structure. More details of the chemical features were supported by Fourier transform infrared (FT-IR) spectroscopy and the results are shown in Figure 3b. All peaks exhibited two main characteristic bands of boron nitride at ≈1365 and 800 cm^{-1} corresponding to in-plane B-N transverse optical mode and out-of-plane B-N-B bending mode, respectively [31]. No major chemical differences could be observed between the samples. Thermal stability of samples was performed in air atmosphere (rate = 10 K/min) and shown in Figure 3c. The TG thermograms

reflected the weight loss of 19% for both samples, representing the removal of moisture adsorbed on the material surface. After 573 K the lines show the thermal stability nature of BN at high temperature and there was no significant weight loss up to 1273 K. The UV-vis absorption collected in Figure 3d indicates a highly transparent from visible to UV wavelength [32]. The maximum absorption peak around 209 nm, is attributed to intrinsic excitation absorption band of h-BN. Besides, small humps around 265 and 352 nm were detected in BN-P123, corresponding to impurities. So far, above all characteristic results on both samples, it was found that the structure and chemical nature of BN has not changed after modifying BN with the surfactant compound and both samples revealed almost similar features. We assumed that the utilisation of block copolymer (P123) might affect the textural properties of pristine BN.

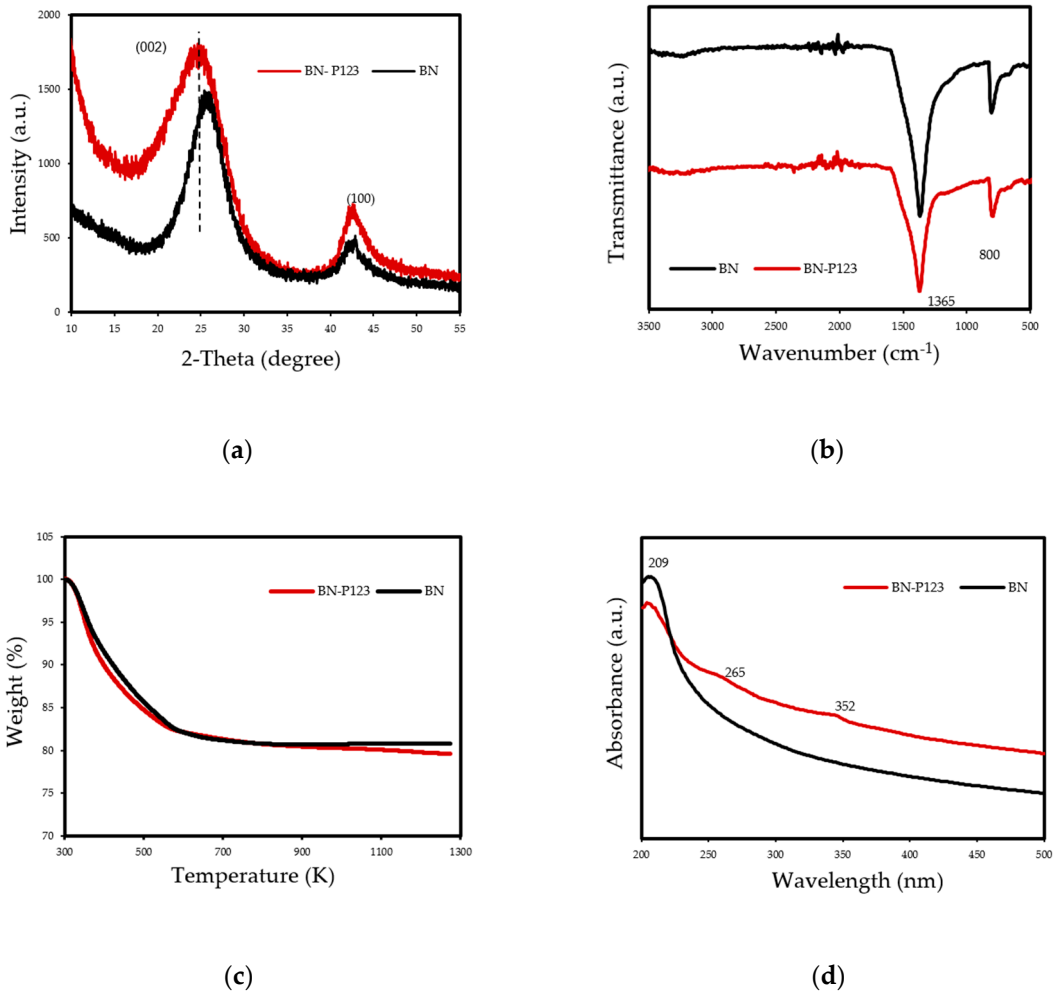

Figure 3. (**a**) XRD patterns; (**b**) FT-IR; (**c**) TG curves and (**d**) UV-Vis of prepared samples.

3.2. Textural Analysis

The textural properties of pristine BN and BN-P123 adsorbent were obtained by nitrogen adsorption/desorption isotherm at 77 K and the results are summarized in Table 1. As indicated in Figure 4a, the resulting isotherms display a typical type II curve based on IUPAC classification and type H3 hystersis loop in the partial pressure range 0.4–1.0, which indicates the presence of mesopores and slit shape pores [33]. There is a trivial rise in N_2 adsorption-desorption isotherm of BN-P123 at lower pressure ($P/P_0 < 0.25$), which is caused by presence of micropores [34]. The non-local density functional theory (NLDFT) was used to calculate pore size distributions. As expected, the dV/dW pore volume of BN-P123 increases dramatically with abundance of micropores (Figure 4b). Meanwhile,

using the Brunauer-Emmett-Teller (BET) method [35], the specific surface areas are calculated showing that the BET surface area of BN-P123 is much higher than pristine BN (Table 1). It is clear from the above measurements that the P123 introduced into precursors during the fabrication process is highly effective on the microscale structure of porous BN and improves surface area and pore volume of the sample.

Table 1. Textural properties and CO_2 capacity (298 K) of prepared materials.

Sample	S_{BET} [1] (m^2/g)	V_{total} [2] (cm^3/g)	CO_2 Uptake (mmol/g)
Pristine BN	102	0.46	2.00
BN-P123	476	0.83	2.69

[1] Specific surface area (m^2/g) obtained by Brunauer-Emmett-Teller (BET) method. [2] Total pore volume (cm^3/g) calculated at P/P_0 = 0.99.

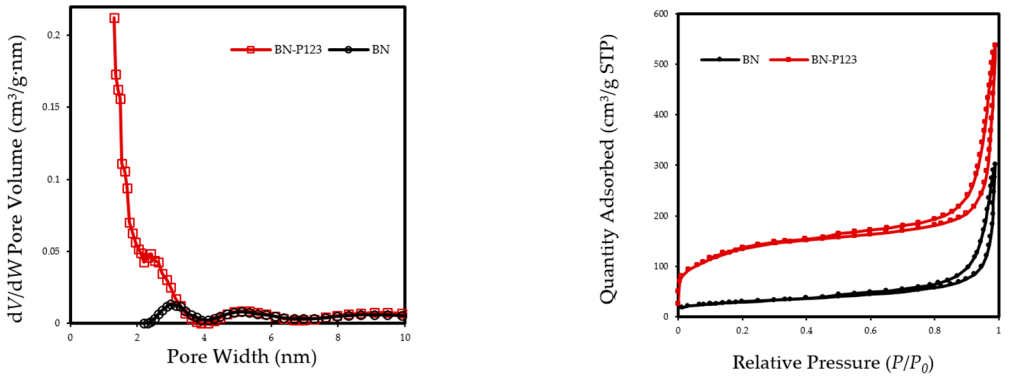

(**a**) (**b**)

Figure 4. (**a**) Nitrogen adsorption-desorption isotherm of the pristine BN and BN-P123; (**b**) NLDFT pore size distribution curves of the same samples.

3.3. Gas Adsorption Analysis

Due to the relatively large porosity of samples, the modified sample BN-P123 and pristine BN were assessed for CO_2 capture under ambient conditions. The adsorption capacities of pure CO_2 on pristine BN and BN-P123 were determined by thermogravimetric analysis. Prior to the sorption test, samples were dried at 393 K with a heating rate of 10 K/min from 298 K under flowing N_2 (150 mL/min) for 6 h and then allowed to cool to the temperature at which the sorption is carried out at 298 K with a heating rate of 10 K/min. When the sorption temperature was reached, samples were stabilized under flowing N_2 (99.99%, 150 mL/min) for 15 min and then N_2 flow was switched to pure CO_2 (99.99%, 50 mL/min) flow for 6 h. The mass uptake during this stage was interpreted as the CO_2 capture capacity. Figures 5 and 6a–c illustrate the setup of experiments and the TG profiles of CO_2 uptake along with weight change results respectively.

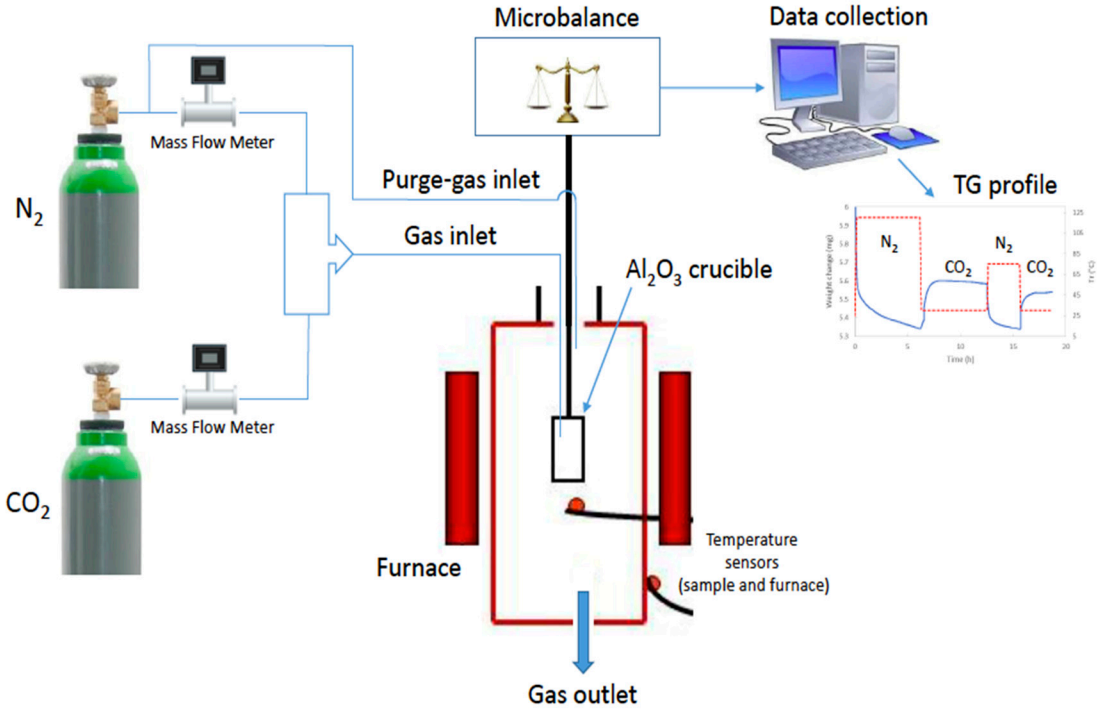

Figure 5. Illustration of CO_2 adsorption experiment.

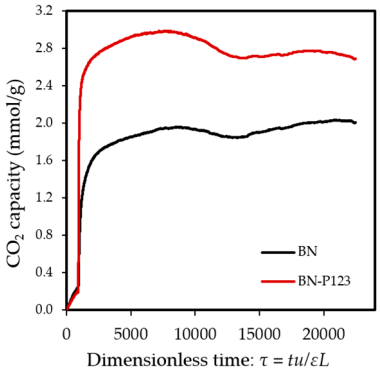

(**a**)

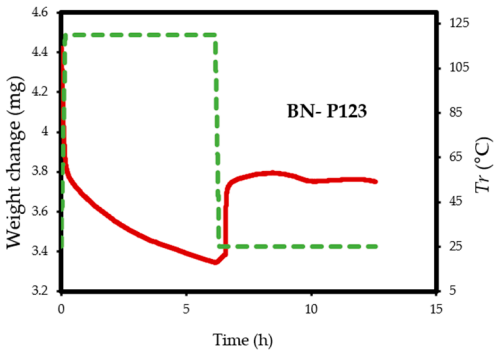

(**b**)

Figure 6. *Cont*

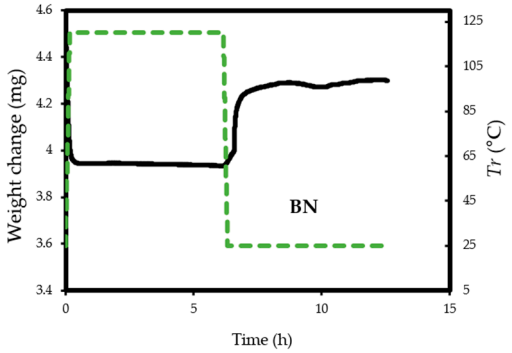

(**c**)

Figure 6. (**a**) TG profiles of CO_2 adsorption on pristine BN and BN-P123; (**b**,**c**) TG profiles of weight change on the same samples.

The experiments reveal that pristine BN shows a CO_2 capacity of 2 mmol/g at 298 K, which enhanced with the addition of P123 copolymer (2.69 mmol/g for BN-P123 at 298 K) (Table 1). The augmented CO_2 adsorption on BN-P123 sample is undoubtedly as a result of the porous morphology of modified BN, whereas pristine BN exhibits lower porosity. It is well-known that higher microporosity provides more active sites and storage space to boost the adsorption performances [36–38]. To the best of our knowledge, the result of the synthetic method is higher than other modification methods such as (3D) BCNO structure (1.8 mmol/g) at 298 K as reported by Lopez-Salas et al. [39] and closer to porous BCN (2.49 mmol/g) at 298 K and porous BN fiber (2.85 mmol/g) at 273 K [40,41]. However, the use of melamine in porous BCN as well as BN fiber leads to the presence of carbon content and consequently decreases the stability upon exposure to ambient air. The effect of high-temperature treatment in different gases was studied in [42], where porous BN fibers treated in NH_3 gas at 1673–1773 K enhanced CO_2 adsorption capacity (from 0.45 mmol/g to 1.6 mmol/g). Nonetheless, this outcome is not a satisfactory result. One possible insight of this finding is that pyrolysis temperature and carrier gas does not lead to a remarkable change in CO_2 uptake. In addition, directing triblock co-polymer was also used to design a hierarchical carbon sorbent [43]. This hierarchical structure is desirable for CO_2 capture as it shows superior capacity (4.5 mmol/g) under ambient conditions. It is noteworthy that at lower pressures (≤1 bar), the density of pore volume, especially the micropores volume plays a critical role in capturing CO_2 [44]. Therefore, high surface area and porosity of BN-P123 has brought about a positive adsorption interaction.

It is to be noted that for the pristine BN (without adding surfactant) the CO_2 adsorption capacity on our sample exceeds those materials reported by Marchesini et al. [45,46]. Although they accomplished highly porous boron nitride with a high surface area (>1900 m^2/g), the CO_2 adsorption capacity of their sample was up to 1.6 mmol/g under ambient condition. Given the results of our approach, one can conclude that though the specific surface area (SSA) is one of the main factors to increase the CO_2 capacity, obtaining a high SSA e.g., (>1000 m^2/g) does not lend itself to an increased CO_2 capacity.

4. Conclusions

In summary, the porosity of boron nitride has been successfully tuned by introducing the triblock copolymer surfactant (P123) during the preparation process of BN precursors. In particular, we found that by utilizing the P123 into boron and nitrogen precursors leads to improved CO_2 adsorption capacity up to 2.69 mmol/g, as compared with pristine porous BN which was found 2.00 mmol/g. Furthermore, based on the structural properties and morphology results obtained in this work, we determine that both samples share almost similar chemical features. However, the porosity of samples revealed a remarkable change and for the sample BN-P123 (0.83 cm^3/g), it was virtually quadrupled as a result of the modification. This significant change is attributed to the formation of more gases during

the decomposition process, thereby creating higher porosity levels. A natural progression of this work is to describe how textural property parameters of BN lead to higher interaction between BN and CO_2 molecules. Our work could be extended by exploring other parameters (e.g., electronic features or surface chemistry of BN), which could influence on BN to capture more CO_2. All in all, our analyses demonstrate the applicability of metal-free modification of BN for enhanced capacity of pure CO_2.

Author Contributions: Main author and synthesized the materials in the laboratory, F.H.; Prepared the original draft, F.H. and M.M.; Performed CO_2 adsorption tests, M.M. and F.D.; 2nd Supervisor and conducted some experiments in her laboratory in TWI, F.H., G.D.; 1st Supervisor, reviewed manuscript, gave comments, edited contents and supervised the PhD student at LSBU, B.S.; All authors have read and agreed to the published version of the manuscript.

Funding: F.H. was partially funded by the School of Engineering, London South Bank University. The Sotacarbo contribution in this work has been carried out within the "Centre of Excellence on Clean Energy" project (CUP: D83C17000370002), funded by the Regional Government of Sardinia (FSC 2014-2020).

Acknowledgments: The authors would like to acknowledge Angelo La Rosa from TWI for running BET adsorption isotherm experiments in the laboratory.

Conflicts of Interest: The authors declare no conflict of interest.

References

1. Oschatz, M.; Antonietti, M. A search for selectivity to enable CO_2 capture with porous adsorbents. *Energy Environ. Sci.* **2018**, *11*, 57–70. [CrossRef]
2. Strielkowski, W.; Lisin, E.; Gryshova, I. Climate policy of the European Union: What to expect from the Paris agreement. *Rom. J. Eur. Aff.* **2016**, *16*, 68.
3. Bui, M.; Adjiman, C.S.; Bardow, A.; Anthony, E.J.; Boston, A.; Brown, S.; Fennell, P.S.; Fuss, S.; Galindo, A.; Hackett, L.A. Carbon capture and storage (CCS): The way forward. *Energy Environ. Sci.* **2018**, *11*, 1062–1176. [CrossRef]
4. Akinpelumi, K.; Saha, C.; Rochelle, G.T. Piperazine aerosol mitigation for post-combustion carbon capture. *Int. J. Greenh. Gas Control* **2019**, *91*, 102845. [CrossRef]
5. Mantripragada, H.C.; Zhai, H.; Rubin, E.S. Boundary dam or Petra nova—Which is a better model for CCS energy supply? *Int. J. Greenh. Gas Control* **2019**, *82*, 59–68. [CrossRef]
6. Lee, S.-Y.; Park, S.-J. A review on solid adsorbents for carbon dioxide capture. *J. Ind. Eng. Chem.* **2015**, *23*, 1–11. [CrossRef]
7. Yang, H.; Xu, Z.; Fan, M.; Gupta, R.; Slimane, R.B.; Bland, A.E.; Wright, I. Progress in carbon dioxide separation and capture: A review. *J. Environ. Sci.* **2008**, *20*, 14–27. [CrossRef]
8. Li, B.; Duan, Y.; Luebke, D.; Morreale, B. Advances in CO_2 capture technology: A patent review. *Appl. Energy* **2013**, *102*, 1439–1447. [CrossRef]
9. Férey, G.; Serre, C.; Devic, T.; Maurin, G.; Jobic, H.; Llewellyn, P.L.; De Weireld, G.; Vimont, A.; Daturi, M.; Chang, J.-S. Why hybrid porous solids capture greenhouse gases? *Chem. Soc. Rev.* **2011**, *40*, 550–562. [CrossRef] [PubMed]
10. Wang, J.; Huang, L.; Yang, R.; Zhang, Z.; Wu, J.; Gao, Y.; Wang, Q.; O'Hare, D.; Zhong, Z. Recent advances in solid sorbents for CO_2 capture and new development trends. *Energy Environ. Sci.* **2014**, *7*, 3478–3518. [CrossRef]
11. Gargiulo, N.; Pepe, F.; Caputo, D. CO_2 adsorption by functionalized nanoporous materials: A review. *J. Nanosci. Nanotechnol.* **2014**, *14*, 1811–1822. [CrossRef]
12. Pardakhti, M.; Jafari, T.; Tobin, Z.; Dutta, B.; Moharreri, E.; Saveh Shemshaki, N.; Suib, S.L.; Srivastava, R. Trends in solid adsorbent materials development for CO_2 capture. *ACS Appl. Mater. Interfaces* **2019**, *11*, 34533–34559. [CrossRef]
13. Yang, S.; Zhan, L.; Xu, X.; Wang, Y.; Ling, L.; Feng, X. Graphene-based porous silica sheets impregnated with polyethyleneimine for superior CO_2 capture. *Adv. Mater.* **2013**, *25*, 2130–2134. [CrossRef] [PubMed]
14. Mendes, P.A.P.; Ribeiro, A.M.; Gleichmann, K.; Ferreira, A.F.P.; Rodrigues, A.E. Separation of CO_2/N_2 on binderless 5A zeolite. *J. CO_2 Util.* **2017**, *20*, 224–233. [CrossRef]
15. Irani, M.; Jacobson, A.T.; Gasem, K.A.M.; Fan, M. Facilely synthesized porous polymer as support of poly(ethyleneimine) for effective CO_2 capture. *Energy* **2018**, *157*, 1–9. [CrossRef]

16. Zhang, J. Design and Synthesis of Metal Organic Frameworks for CO_2 Separation and Catalysis. Ph.D. Thesis, Rutgers University, Newark, NJ, USA, 2013.
17. Cota, I.; Martinez, F.F. Recent advances in the synthesis and applications of metal organic frameworks doped with ionic liquids for CO_2 adsorption. *Coord. Chem. Rev.* **2017**, *351*, 189–204. [CrossRef]
18. Ello, A.S.; de Souza, L.K.C.; Trokourey, A.; Jaroniec, M. Coconut shell-based microporous carbons for CO_2 capture. *Microporous Mesoporous Mater.* **2013**, *180*, 280–283. [CrossRef]
19. Weng, Q.; Wang, X.; Wang, X.; Bando, Y.; Golberg, D. Functionalized hexagonal boron nitride nanomaterials: Emerging properties and applications. *Chem. Soc. Rev.* **2016**, *45*, 3989–4012. [CrossRef]
20. Shtansky, D.V.; Firestein, K.L.; Golberg, D. V Fabrication and application of BN nanoparticles, nanosheets and their nanohybrids. *Nanoscale* **2018**, *10*, 17477–17493. [CrossRef]
21. Sun, Q.; Li, Z.; Searles, D.J.; Chen, Y.; Lu, G.; Du, A. Charge-controlled switchable CO_2 capture on boron nitride nanomaterials. *J. Am. Chem. Soc.* **2013**, *135*, 8246–8253. [CrossRef]
22. Choi, H.; Park, Y.C.; Kim, Y.-H.; Lee, Y.S. Ambient carbon dioxide capture by boron-rich boron nitride nanotube. *J. Am. Chem. Soc.* **2011**, *133*, 2084–2087. [CrossRef] [PubMed]
23. Owuor, P.S.; Park, O.-K.; Woellner, C.F.; Jalilov, A.S.; Susarla, S.; Joyner, J.; Ozden, S.; Duy, L.; Villegas Salvatierra, R.; Vajtai, R. Lightweight hexagonal boron nitride foam for CO_2 absorption. *ACS Nano* **2017**, *11*, 8944–8952. [CrossRef] [PubMed]
24. Nag, A.; Raidongia, K.; Hembram, K.P.S.S.; Datta, R.; Waghmare, U.V.; Rao, C.N.R. Graphene analogues of BN: Novel synthesis and properties. *ACS Nano* **2010**, *4*, 1539–1544. [CrossRef] [PubMed]
25. Xiao, F.; Chen, Z.; Casillas, G.; Richardson, C.; Li, H.; Huang, Z. Controllable synthesis of few-layered and hierarchically porous boron nitride nanosheets. *Chem. Commun.* **2016**, *52*, 3911–3914. [CrossRef]
26. Chen, Y.; Wang, J.; Chen, Y.; Liu, D.; Huang, S.; Lei, W. One-step template-free synthesis of 3D functionalized flower-like boron nitride nanosheets for NH3 and CO_2 adsorption. *Nanoscale* **2018**, *10*, 10979–10985.
27. Chen, S.; Li, P.; Xu, S.; Pan, X.; Fu, Q.; Bao, X. Carbon doping of hexagonal boron nitride porous materials toward CO_2 capture. *J. Mater. Chem. A* **2018**, *6*, 1832–1839. [CrossRef]
28. Huang, K.; Liang, L.; Chai, S.; Tumuluri, U.; Li, M.; Wu, Z.; Sumpter, B.G.; Dai, S. Aminopolymer functionalization of boron nitride nanosheets for highly efficient capture of carbon dioxide. *J. Mater. Chem. A* **2017**, *5*, 16241–16248. [CrossRef]
29. Xiong, J.; Yang, L.; Chao, Y.; Pang, J.; Zhang, M.; Zhu, W.; Li, H. Boron nitride mesoporous nanowires with doped oxygen atoms for the remarkable adsorption desulfurization performance from fuels. *ACS Sustain. Chem. Eng.* **2016**, *4*, 4457–4464. [CrossRef]
30. Kurakevych, O.O.; Solozhenko, V.L. Rhombohedral boron subnitride, B13N2, by X-ray powder diffraction. *Acta Crystallogr. Sect. C Cryst. Struct. Commun.* **2007**, *63*, i80–i82. [CrossRef]
31. Liu, F.; Yu, J.; Ji, X.; Qian, M. Nanosheet-structured boron nitride spheres with a versatile adsorption capacity for water cleaning. *ACS Appl. Mater. Interfaces* **2015**, *7*, 1824–1832. [CrossRef]
32. Ba, K.; Jiang, W.; Cheng, J.; Bao, J.; Xuan, N.; Sun, Y.; Liu, B.; Xie, A.; Wu, S.; Sun, Z. Chemical and bandgap engineering in monolayer hexagonal boron nitride. *Sci. Rep.* **2017**, *7*, 45584. [CrossRef] [PubMed]
33. Pang, J.; Chao, Y.; Chang, H.; Li, H.; Xiong, J.; Zhang, Q.; Chen, G.; Qian, J.; Zhu, W.; Li, H. Silver nanoparticle-decorated boron nitride with tunable electronic properties for enhancement of adsorption performance. *ACS Sustain. Chem. Eng.* **2018**, *6*, 4948–4957. [CrossRef]
34. Bi, W.; Hu, Y.; Li, W.; Jiang, H.; Li, C. Construction of nanoreactors combining two-dimensional hexagonal boron nitride (h-BN) coating with Pt/Al_2O_3 catalyst toward efficient catalysis for CO oxidation. *Ind. Eng. Chem. Res.* **2018**, *57*, 13353–13361. [CrossRef]
35. Brunauer, S.; Emmett, P.H.; Teller, E. Adsorption of gases in multimolecular layers. *J. Am. Chem. Soc.* **1938**, *60*, 309–319. [CrossRef]
36. Li, J.; Xiao, X.; Xu, X.; Lin, J.; Huang, Y.; Xue, Y.; Jin, P.; Zou, J.; Tang, C. Activated boron nitride as an effective adsorbent for metal ions and organic pollutants. *Sci. Rep.* **2013**, *3*, 3208. [CrossRef]
37. Xiong, J.; Li, H.; Yang, L.; Luo, J.; Chao, Y.; Pang, J.; Zhu, W. Metal-free boron nitride adsorbent for ultra-deep desulfurization. *AIChE J.* **2017**, *63*, 3463–3469. [CrossRef]
38. Liu, F.; Li, S.; Yu, D.; Su, Y.; Shao, N.; Zhang, Z. Template-free synthesis of oxygen-doped bundlelike porous boron nitride for highly efficient removal of heavy metals from wastewater. *ACS Sustain. Chem. Eng.* **2018**, *6*, 16011–16020. [CrossRef]

39. López-Salas, N.; Ferrer, M.L.; Gutiérrez, M.C.; Fierro, J.L.G.; Cuadrado-Collados, C.; Gandara-Loe, J.; Silvestre-Albero, J.; del Monte, F. Hydrogen-bond supramolecular hydrogels as efficient precursors in the preparation of freestanding 3D carbonaceous architectures containing BCNO nanocrystals and exhibiting a high CO_2/CH_4 adsorption ratio. *Carbon N. Y.* **2018**, *134*, 470–479. [CrossRef]
40. Florent, M.; Bandosz, T.J. Irreversible water mediated transformation of BCN from a 3D highly porous form to its nonporous hydrolyzed counterpart. *J. Mater. Chem. A* **2018**, *6*, 3510–3521. [CrossRef]
41. Wang, D.; Xue, Y.; Wang, C.; Ji, J.; Zhou, Z.; Tang, C. Improved capture of carbon dioxide and methane via adding micropores within porous boron nitride fibers. *J. Mater. Sci.* **2019**, *54*, 10168–10178. [CrossRef]
42. Liang, J.; Song, Q.; Lin, J.; Huang, Y.; Fang, Y.; Yu, C.; Xue, Y.; Liu, Z.; Tang, C. Pore structure regulation and carbon dioxide adsorption capacity improvement on porous BN fibers: Effects of high-temperature treatments in gaseous ambient. *Chem. Eng. J.* **2019**, *373*, 616–623. [CrossRef]
43. To, J.W.F.; He, J.; Mei, J.; Haghpanah, R.; Chen, Z.; Kurosawa, T.; Chen, S.; Bae, W.-G.; Pan, L.; Tok, J.B.-H. Hierarchical N-doped carbon as CO_2 adsorbent with high CO_2 selectivity from rationally designed polypyrrole precursor. *J. Am. Chem. Soc.* **2016**, *138*, 1001–1009. [CrossRef] [PubMed]
44. Li, Y.; Ben, T.; Zhang, B.; Fu, Y.; Qiu, S. Ultrahigh gas storage both at low and high pressures in KOH-activated carbonized porous aromatic frameworks. *Sci. Rep.* **2013**, *3*, 2420. [CrossRef] [PubMed]
45. Marchesini, S.; Regoutz, A.; Payne, D.; Petit, C. Tunable porous boron nitride: Investigating its formation and its application for gas adsorption. *Microporous Mesoporous Mater.* **2017**, *243*, 154–163. [CrossRef]
46. Marchesini, S.; McGilvery, C.M.; Bailey, J.; Petit, C. Template-free synthesis of highly porous boron nitride: Insights into pore network design and impact on gas sorption. *ACS Nano* **2017**, *11*, 10003–10011. [CrossRef] [PubMed]

© 2020 by the authors. Licensee MDPI, Basel, Switzerland. This article is an open access article distributed under the terms and conditions of the Creative Commons Attribution (CC BY) license (http://creativecommons.org/licenses/by/4.0/).